NASA TECHNICAL NOTE

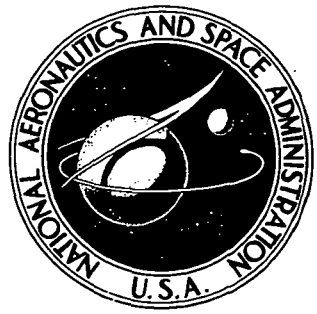

NASA TN D-7125

NASA TN D-7125

SINGLE-THRUST-PERIOD MISSIONS TO URANUS FOR UNMANNED NUCLEAR-ELECTRIC PROPULSION SYSTEMS

by Charles L. Zola

Lewis Research Center
Cleveland, Ohio 44135

NATIONAL AERONAUTICS AND SPACE ADMINISTRATION • WASHINGTON, D. C. • JANUARY 1973

1. Report No.	2. Government Accession No.	3. Recipient's Catalog No.
NASA TN D-7125		

4. Title and Subtitle	5. Report Date
SINGLE-THRUST-PERIOD MISSIONS TO URANUS FOR UNMANNED NUCLEAR-ELECTRIC PROPULSION SYSTEMS	January 1973
	6. Performing Organization Code

7. Author(s)	8. Performing Organization Report No.
Charles L. Zola	E-6839
	10. Work Unit No.
9. Performing Organization Name and Address	501-04
Lewis Research Center National Aeronautics and Space Administration Cleveland, Ohio 44135	11. Contract or Grant No.
	13. Type of Report and Period Covered
12. Sponsoring Agency Name and Address	Technical Note
National Aeronautics and Space Administration Washington, D.C. 20546	14. Sponsoring Agency Code

15. Supplementary Notes

16. Abstract

The effects of trip time, propulsion time, and specific powerplant mass are studied for optimized unmanned probe spacecraft on missions to Uranus with nuclear-electric propulsion systems. Electric propulsion is confined to a single thrust period at the beginning of each mission. Mission profiles include both high-thrust and electric-propulsion Earth-departure modes for planet flyby and orbital capture. Effects of propulsion time and propulsion system parameters are evaluated, and typical design features of the nuclear-electric spacecraft are outlined. Payload capability comparisons are made with systems employing ballistic transfer and solar-electric propulsion.

17. Key Words (Suggested by Author(s))	18. Distribution Statement
Interplanetary; Nuclear-electric powerplants; Nuclear-electric propulsion; Unmanned; Uranus; Outer planets; Launch vehicles; Electric propulsion spacecraft; Ion thruster; Trajectories; Flyby; Capture	Unclassified - unlimited

19. Security Classif. (of this report)	20. Security Classif. (of this page)	21. No. of Pages	22. Price*
Unclassified	Unclassified	35	$3.00

* For sale by the National Technical Information Service, Springfield, Virginia 22151

CONTENTS

SINGLE-THRUST-PERIOD MISSIONS TO URANUS FOR UNMANNED NUCLEAR-ELECTRIC PROPULSION SYSTEMS

by Charles L. Zola

Lewis Research Center

SUMMARY

This report evaluates the performance potential of unmanned nuclear-electric propulsion spacecraft for orbiter and flyby probe missions to Uranus. A single electric-propulsion phase is allowed at the beginning of each mission trajectory and, for capture missions, a chemical-propulsion retrorocket is used for orbit insertion at Uranus. Both spiral and boosted escape maneuvers are considered at Earth departure. Either the Titan IIID(7) or the Space Shuttle is used to launch the electric-propulsion spacecraft to orbit. A Centaur is used, if needed, as an upper stage to boost the spacecraft into a high-energy Earth escape path. Free parameters, such as electric-propulsion power level and thruster specific impulse, are optimized to maximize payload capability.

Results are presented to show the effects of trip time, propulsion time, and power-plant specific mass on payloads and on optimum specific impulse and installed power. For reasonable payloads, mission trip times must be greater than 1500 days for flyby missions, or greater than 2500 days for capture missions. Propulsion time, however, need not be greater than 400 to 800 days for any case considered. For capture missions, optimum propulsion times occur at 400 to 600 days.

It is found that the single-thrust-period propulsion profile yields payload performance approaching that of the optimum, but complex, thrust-coast-thrust profile. Therefore, it is concluded that the single thrust period is a reasonable operational mode for a nuclear-electric propulsion system, based on a modest development program.

Payload capability comparisons are made with all-ballistic and solar-electric propulsion modes. When based on the same launch vehicle, the study shows that the nuclear-electric system is capable of more payload than solar-electric systems at short mission times, but the performance of the two systems becomes comparable at longer trip times. When compared with the ballistic-mission-mode alternative, nuclear-electric systems show significant payload advantage over a wide range of mission trip times, although the nuclear-electric and ballistic modes become identical at extremely short mission times.

INTRODUCTION

An electric-propulsion system is attractive because of its high specific impulse. In principle, it consists of two main elements: thrusters and powerplant. Thruster technology is progressing rapidly toward readiness for primary propulsion applications, as witnessed by the SERT II demonstration (ref. 1) and by current research programs (ref. 2).

A solar-electric powerplant suitable for low-powered (20 kW or under) applications could be derived from current or near-future technology (ref. 3) and the resultant vehicle would offer an attractive range of mission capabilities (refs. 4 and 5 to 7). But for large-vehicle, high-power applications, projected nuclear-electric systems (cf. refs. 8 to 25) could be both lighter and less costly. Nuclear-electric systems can be especially attractive for outer-planet missions because they maintain a constant power output - whereas solar-electric systems experience a severe (e.g., inverse-square) power falloff with increasing solar distance. Considerable further development will be required, however, to bring nuclear-electric systems to flight-readiness. At present, there is a definite need to set attainable goals for technology in the areas of system weight and operating life which will be useful in mission applications.

This report examines the performance potential and advantageous design characteristics of nuclear-electric propulsion for flyby and orbiter probe missions, using Uranus as a typical destination among the outer planets. As an example of applications for early or first-generation propulsion systems, the present study makes use of moderate power levels and a simplified operating profile (thrusting limited to a single relatively brief period at the beginning of each trajectory). Relatively low-cost, intermediate-size launch vehicles are used: either Titan IIID(7) or the Space Shuttle, plus Centaur if needed for an upper stage. By contrast, most previous studies have adopted the more efficient, but more complex, thrust-coast-thrust profile for orbiter missions. The major exception (ref. 11) assumed a completely high-thrust launch using Saturn V plus two new chemical upper stages. This was to be followed, after an appropriate coast period, by a single phase of electric thrusting at the end of the mission, during the period just before planet encounter. Although not requiring a restartable system, this approach involved the same environmental hazards and had the same needs for environmental protection (e.g., radiator armor) as the thrust-coast-thrust profile. Moreover, by the use of Saturn V, it implied high launch costs and high electric power outputs to be commensurate with Saturn V's load-lifting capacity.

In this report, Earth-to-Uranus flyby and capture missions are examined parametrically for the following conditions:

(1) Trip time, T, 1000 to 4000 days

(2) Propulsion time, t_p, 200 to 800 days

(3) Powerplant specific mass, α, 10 to 40 kg/kW

The consequent performance (as measured by delivered payload) is compared with that obtainable with the optimum thrust-coast-thrust trajectory profile, and also with all-ballistic and solar-electric propulsion results.

ANALYSIS

Mission Profiles

Four different electric-propulsion mission profiles are described in this section. These are (1) initial-spiral flyby, (2) initial-spiral capture, (3) boosted flyby, and (4) boosted capture. The following parts of the analysis will define and explain these terminologies and describe the calculation procedures, input assumptions, and constraints incorporated in generating the data given in the section RESULTS AND DISCUSSION.

Earth departure. - In initial-spiral mission profiles, the electric spacecraft escapes Earth from a low circular orbit under its own power by following a low-thrust spiral trajectory. For "boosted" mission profiles an additional chemical launch stage places the electric spacecraft on a high-energy Earth escape path.

The Titan IIID(7) is the basic launch vehicle for each electric-propulsion mission profile. In terms of payload delivered to Earth orbit, the performance of the Titan IIID(7) is less than the maximum capability expected for the Space Shuttle. However, the two launch systems are comparable, especially in the case of an off-loaded Shuttle. Therefore, the results to be shown subsequently can be considered as representative of Shuttle-launched nuclear-electric propulsion systems. For initial spiral profiles, the Titan IIID(7), or Shuttle, places the electric spacecraft in a 185-kilometer-altitude Earth orbit. In boosted mission profiles, the electric spacecraft is launched by a Titan IIID(7)/Centaur or a Shuttle/Centaur.

The single allowed electric-propulsion phase takes place after the launch phase. For initial-spiral missions, the allowed propulsion time must include the time required by the Earth escape spiral and the time spent thrusting in heliocentric space. In boosted mission profiles, all the allotted propulsion time is used in heliocentric space at the Earth end of the Earth-Uranus trajectory. In all cases, the spacecraft is coasting at Uranus encounter.

Uranus encounter. - The second major difference in mission profile depends on whether the spacecraft performs a flyby encounter or is captured in a parking orbit at Uranus. Both the boosted and initial-spiral Earth departure alternatives are applied to flyby and capture Uranus encounters to result in the four different mission profiles mentioned previously.

In capture missions a chemical-propulsion retrorocket is assumed to place the payload in a loose elliptical orbit about the planet. The capture orbit arbitrarily chosen for

this study has a periapsis of 2 planet radii and an apoapsis of 38 planet radii (2×38). For Uranus, this orbit has a period of about 10 days.

The retrorocket system is assumed to have a specific impulse of 420 seconds and an associated hardware (tankage, etc.) of 15 percent of the retropropellant loading. The entire electric-propulsion system (powerplant, thrusters, tankage, etc.) is jettisoned, or separated, from the payload prior to the retropropulsion maneuver. The jettison is necessary because of the high propellant requirements (to be shown later) of the chemical retrorocket system. In most cases to be presented, no payload would be possible without such jettisoning. At best, the powerplant could be captured but with no weight allowance for sensor and communication systems which could use it. The alternative of using the electric-propulsion system for capture maneuvers calls for a longer-life restartable powerplant.

Trajectory Computation

The mission trajectories for this report are calculated with the Lewis N-Body Code (ref. 26), a general-purpose digital computer program for the calculation of spaceflight trajectories. The feature of the code used in this study is the solution of boundary-value problems in optimal (minimum propellant requirement) trajectories for constant-thrust, constant-specific-impulse propulsion systems. The trajectory code includes a calculus-of-variations technique to determine optimum thrust periods and an optimum steering schedule for the thrust vector to minimize propellant requirement. For the present study, the code was modified to limit the electric-propulsion phase to a single period at the beginning of each trip.

To avoid complexity, the trajectory calculations in this study assume a two-dimensional solar system with Earth and Uranus in circular orbits at their mean distances from the Sun. This is a satisfactory approximation for missions to Uranus since its orbital eccentricity is 0.05 (ref. 27) and the inclination of its orbit to the ecliptic is only 0.77 degree. Furthermore, each integrated heliocentric trajectory is assumed to be a "two-body" trajectory, in which the spacecraft motion is affected only by the Sun and the thrust. The assumed constants for the planetary model are the following (ref. 27):

	Earth	Uranus
Mean distance from Sun, m	1.49599×10^{11}	2.88020×10^{12}
Mean orbital velocity, m/sec	2.977×10^{4}	6.797×10^{3}
Radius of planet, m	6.378×10^{6}	2.350×10^{7}
Gravitational constant, m^3/sec^2	3.986×10^{14}	5.788×10^{15}

Necessary input parameters for each mission trajectory calculation include the planetary data from the preceding table, the desired trip time T, and the allowed electric-propulsion time t_p. Other important input parameters are the ratio of power to initial mass of the nuclear-electric spacecraft P/m_0, the specific impulse of the electric thruster system I_{sp}, and the powerplant specific mass α. For boosted mission profiles, a value of low-Earth-altitude injection velocity must be specified for the electric spacecraft. In such cases, parameters describing the characteristics of the launch vehicle are also included to determine the initial mass of the nuclear-electric spacecraft at each specified injection velocity.

Each mission trajectory solution provides a history of the position, velocity, and thrust vector control schedule of the low-thrust spacecraft. The spacecraft mass delivered to planet encounter and the propellant requirement of the electric-propulsion system are determined from the mass history of each case. For capture missions, the trajectory encounter velocity, the desired parking-orbit ellipse, and the input parameters of the retropropulsion rocket determine the mass requirement of the braking rocket system. The delivered payload can then be calculated by accounting for the mass required for the propellant, the propulsion system, and (if any) the braking rocket system. (As used herein, the "payload" of the spacecraft is any mass not allocated to propellants, propulsion systems, or tankage.) In each case, the delivered payload is maximized by optimizing such parameters as propulsion system power, thruster specific impulse, and (if appropriate) launch velocity at low Earth altitude.

Launch Vehicles

Examples of Titan IIID(7) and Shuttle launch vehicle payloads for injection velocities at low Earth altitude are given in figure 1. Due-East launches from the Eastern Test Range (ETR) are assumed in the figure. Performance characteristics of the Titan IIID(7) and Titan IIID(7)/Centaur systems were obtained from reference 28. Baseline Shuttle and Shuttle/Centaur performance objectives are taken from references 29 and 30. The characteristic injection velocity V_B in figure 1 is the equivalent velocity that the launch vehicle payload could be given at 185-kilometer (100-n mi) perigee altitude. At that altitude, circular orbit velocity is about 7.8 km/sec and Earth escape velocity is about 11 km/sec, as noted in the figure. The Titan IIID(7) alone is used in initial-spiral missions to launch the electric-propulsion spacecraft into a circular Earth orbit at 185 kilometers. The orbital payload capability of 17 300 kilograms, noted in figure 1 at a characteristic injection velocity of 7.8 km/sec, is the initial mass of the electric spacecraft for initial-spiral profiles.

In boosted mission profiles, the payload of the Titan IIID(7)/Centaur launch vehicle (i.e., the initial mass of the electric-propulsion spacecraft) varies from 7400 kilograms at Earth escape speed (11 km/sec) to lower values as the injection velocity is raised.

The Space Shuttle is a reusable launch vehicle concept presently under development by NASA. Performance of a baseline configuration of the Shuttle which is consistent with current requirements of the Space Shuttle Program Office (ref. 29) is included in figure 1, showing a 29 000-kilogram maximum orbital payload capability without upper stages at the equivalent injection velocity of 7.8 km/sec. In addition, maximum payload capability of the Shuttle/Centaur launch vehicle (ref. 30) at injection velocities above escape speed are shown in figure 1 with a dashed curve. The launch capability curve of the Shuttle/Centaur is very similar to the Titan IIID(7)/Centaur curve, with the Shuttle-based system having about 30 percent greater capability at each V_B. Therefore, mission performance (to be discussed later) based on Titan IIID(7) launch vehicles could be equaled or exceeded by the use of Shuttle-based launch systems. However, the nuclear-electric spacecraft with Centaur must integrate with the 4.5-meter by 18.3-meter (15-ft by 60-ft) cargo bay of the Shuttle.

Propulsion System

As previously mentioned, the two main elements of an electric-propulsion system are the powerplant and the thrusters. The powerplant, in most cases, comprises nearly all the propulsion system's weight. The thrusters are light in comparison, but they determine how effectively the energy generated by the powerplant is converted to useful thrust. For the purposes of the present study, thruster system weight is assumed to be included in the powerplant weight.

Powerplants. - Powerplant mass depends primarily on the power level, the type of reactor and conversion equipment, and the assumed state of technology. Figure 2 shows the relations between power and mass from a representative group of design studies. Of the systems illustrated, only two - the SNAP-8 at 35 kilowatts and the Isotope-Brayton at 10 kilowatts - have ever reached a hardware stage.

Although some man-rated systems are included for comparison (diamond symbols), the primary interest herein is the less-heavily shielded, "instrument rated" (i.e., unmanned) systems. These are denoted by circular symbols, with recent studies being solid symbols and the older ones open symbols. Details of each study can be found in the indicated references and will not be further discussed herein. In summary, it appears that, with perhaps one exception (ref. 24), the more recent references indicate that the powerplant specific mass α will lie between 10 and 40 kg/kW.

Thrusters. - Figure 3 shows typical efficiency curves and data for ion thrusters as a function of specific impulse I_{sp}. Due to inherent energy losses, the efficiency of the thruster η_{th} decreases with decreasing specific impulse. Thruster size and state-of-the-art considerations also affect the efficiency. The 15-centimeter-diameter SERT II thruster performance, given in reference 1, is noted at one point in figure 3. Figure 3 also includes data, taken from reference 2, for present (1971) and expected future (1980) performance of 30- and 150-centimeter-diameter thrusters. For comparison purposes the figure includes a curve (also taken from ref. 2) to represent the efficiency of "ideal" hypothetical mercury-ion thrusters whose energy losses have been reduced to a practical minimum. Efficiency goals (1980) for the 30-centimeter-diameter thrusters are placed very near the ideal curve in figure 3. For the 150-centimeter-diameter thruster, expected future efficiencies fall below the ideal curve because development of this thruster has been subordinated to other programs (ref. 2) since 1968.

The present study uses the curve labeled "Projected technology" in figure 3 to represent overall thruster efficiency for future large thrusters. This hypothetical efficiency curve is shaped such that it slightly exceeds the performance of current 30-centimeter-diameter thrusters and matches the expected future performance of the 150-centimeter-diameter thruster.

The present study also assumes that a 93-percent-efficient power conditioning system is required for the ion thruster system. Hence, overall efficiency of the propulsion system is 93 percent of the thruster efficiency given in figure 3.

RESULTS AND DISCUSSION

Effect of Trip Time, Propulsion Time, and Powerplant Specific Mass

The numerical results of this study are presented by illustrating the effects of trip time T, propulsion time t_p, and powerplant specific mass α on payload and the optimum values of specific impulse, launch velocity, and electric-propulsion system power level. Boosted flyby and capture missions are treated in the first two sections. Results for initial-spiral flyby and capture missions are covered in the last two sections.

Boosted flyby mission. - Figure 4 is presented in four parts to summarize the effect of trip time on payload, power level, launch velocity, and specific impulse of optimally designed, boosted nuclear-electric spacecraft for Uranus flyby missions. Results are shown for combinations of two values of t_p and two values of α. In addition, figures 5 and 6 show the effect of t_p and α directly on the same four parameters, for fixed trip times of 1500 and 2500 days, respectively.

As shown in figure 4(a), longer trip time tends to increase the payload capability for each fixed combination of t_p and α, although the curves flatten as trip time T increases. However, for α of 20 or 40 kg/kW, there is no major difference between payloads for a t_p of 800 or 400 days for a wide range of trip times. The same trends can be observed in figures 5(a) and 6(a) for fixed trip times. This illustrates that, although longer t_p improves flyby payload capability, a nuclear-electric propulsion system with as little as 10 000 hours ($\approx$400 days) of lifetime and no restart capability can yield a useful level of performance.

Optimum power levels, as shown in figures 4(b), 5(b), and 6(b), are in the range of 80 to 100 kilowatts for an α of 20 kg/kW and 30 to 60 kilowatts for an α of 40 kg/kW. Only a modest-sized powerplant is needed. The figures show that although t_p does not have a strong effect on power requirement at each given trip time, α can have a major effect. The similarities in power level when only t_p is varied result from proportionate increases in I_{sp} and decreases in thrust as longer t_p is allowed. The lower power levels for an α of 40 kg/kW are the result not only of lower values of optimum I_{sp} but also of generally lower values of total mass for the electric-propulsion spacecraft. These lower values of total mass result from higher optimum launch velocities at each trip time. It is interesting to note that the effect of α on optimum power level tends to keep the mass of the powerplant more constant than the power level. For example, in figures 5(b) and 6(b), the powerplant mass, given by αP, varies only between 1000 and 2000 kilograms although optimum power levels range from 30 kilowatts to more than 130 kilowatts.

At relatively short trip times (near 1000 days), all cases show a decrease in optimum power level because of increases in optimum launch velocity, which result in lower spacecraft total mass. On the other hand, optimum system power level can also decrease at longer trip times because thrust requirements are lower even though spacecraft total mass increases. In the cases shown in figure 4(b), optimum power level actually maximizes near trip times of 1500 days when α is 20 kg/kW and 2500 days when α is 40 kg/kW.

From figure 4(c), it can be seen that shorter trip times always lead to increased launch velocity. The principal reason for this effect is that shorter trip times have high propulsive requirements Δv in contrast to the capability of the electric-propulsion system. Trade-offs to maximize payload as trip time is reduced lead to a diminishing size for the electric-propulsion system with an increase in optimum launch velocity until, eventually, the optimum mission design is "all ballistic," having no electric-propulsion system.

For an α of 20 kg/kW, increasing trip time decreases the optimum launch velocity toward the Earth escape value (11 km/sec), which is the minimum possible launch velocity for an electric spacecraft in the boosted mission mode. However, the combination of shorter propulsion time (400 days) and heavier powerplant weight (40 kg/kW) requires considerably higher launch velocities, even at relatively long trip times (see fig. 4(c)).

Optimum specific impulse in figure 4(d) is almost unaffected by trip time. However, it is apparent from figures 5(d) and 6(d) that optimum I_{sp} varies directly with t_p and inversely with α, such that combinations of low α and high t_p result in the highest optimum I_{sp}. This corresponds with previous analytic studies of electric-propulsion-system performance, such as reference 31, which have shown that optimum I_{sp} depends on $\sqrt{t_p/\alpha}$.

Boosted capture missions. - Figures 7 and 8 summarize the effect of trip time, powerplant specific mass, and propulsion time on the important parameters of optimally designed nuclear-electric spacecraft for boosted Uranus capture missions. In general, the trends shown in figure 7 for variations in payload, optimum installed power, optimum launch velocity, and optimum specific impulse are similar to those in the flyby mission data presented in figure 4. Capture mission payloads are, however, much less than the payloads possible on flyby missions for any given trip time. Capture payloads in the range of 1000 to 2000 kilograms require trip times of 2500 to 3500 days. Flyby missions with payloads in the same range require only 1100 to 1500 days.

The occurrence of optimum propulsion times is the major difference between the capture mission results (figs. 7 and 8) and the flyby mission results (figs. 4 to 6). Figures 7(a) and 8(a) show that, for an α of 20 kg/kW, a 400-day propulsion time can result in better payload than an 800-day propulsion time for most trip times below 4000 days. In fact, as shown in figure 8(a), the optimum propulsion time is roughly 400 days for the 2500-day capture mission, regardless of the value of α. This is because long propulsion times tend to result in high planet-approach velocities and, hence, high retropropellant requirements.

As can be seen by comparing figures 8(a) and (c), the maximum payload condition (for a given α) corresponding to optimum t_p is nearly coincident with minimum launch velocity, that is, with maximum spacecraft initial mass.

As in the previous mission profile, the optimum power level varies slowly with trip time and t_p and rapidly with α (figs. 7(b) and 8(b)). Optimum specific impulse is insensitive to trip time, as shown in figure 7(d), but varies significantly with t_p and α, as shown in figure 8(d).

Initial-spiral flyby missions. - Initial-spiral flyby and capture mission results are presented in this, and the following, section in a similar manner to the previous sections concerning the boosted mode. The effects of T, t_p, and α on payload, optimum power level, and optimum specific impulse are shown in figures 9 to 12. There is no discussion of optimum launch velocity since this parameter does not apply to the initial-spiral mode. All missions start in low Earth orbit with an initial mass of 17 300 kilograms. The propulsion times and trip times cited in the data for the initial-spiral mode include the time required to escape from low Earth orbit by using the electric-propulsion system. This spiral time varies from case to case, ranging between 100 and 300 days.

Figures 9 and 10 summarize initial-spiral nuclear-electric Uranus flyby missions by showing the effect of trip time on payload, optimum power level, and optimum specific impulse. Propulsion times of 400 and 800 days are combined with values of α of 20 and 40 kg/kW.

The payload curve in figure 9(a) exhibits the usual increase with trip time for any combination of t_p and α, along with a tendency to decrease in slope at the higher trip times. The curves do not cross over one another, indicating (as is also illustrated in fig. 10(a)) that the longer the t_p or lower the α, the greater will be the payload. Decreasing the allowed propulsion time from 800 to 400 days has less effect than an increase in α from 20 to 40 kg/kW.

Figures 9(b) and (c) show a tendency to higher optimum power levels and lower optimum specific impulse as trip time is decreased. These trends in power and specific impulse result from a need for higher thrust from the electric-propulsion system as trip time is shortened. However, for the trip-time range which yields relatively good payloads (e.g., above 2500 days in fig. 9(a)), power and specific impulse remain fairly constant for given values of t_p and α, as shown in figures 9(b) and (c). Optimum specific-impulse values (for various combinations of t_p and α) in figure 9(c) are similar to those for the boosted mission profiles in earlier figures.

As shown in the previous discussion of boosted mission profiles, the range in optimum power level for initial-spiral missions shown in figures 9(b) and 10(b) is greater than the range in powerplant mass, since the power levels increase as α decreases. Powerplant mass ranges from 4300 to 6000 kilograms for all the cases covered in figure 9. This means that the powerplant mass optimizes at 25 to 35 percent of the fixed 17 300-kilogram spacecraft total mass.

Optimum installed power is three to five times the amount needed for boosted missions. This is mostly caused by the fact that the total mass of spiral-mode spacecraft is three to five times the total mass of the spacecraft launched at high velocity on boosted missions.

Initial-spiral capture missions. - Data are presented in figures 11 and 12 for nuclear-electric capture missions to Uranus, using the initial-spiral mode. In figure 11, the effect of trip time on payload, optimum installed power, and optimum specific impulse is shown for several selected combinations of propulsion time and powerplant specific mass. Data for t_p greater than 600 days are not included in figure 11 because longer propulsion times are generally not optimum in the trip-time range below 3500 days. The range of trip time covered in figure 11 is smaller than that for the flyby mission data in figure 9 since, as shown in figure 11(a), even the best cases drop to very small payloads at 2200- to 2400-day trip times.

Optimum system power levels shown in figure 11(b) for initial-spiral capture missions are almost identical to those for initial-spiral flyby missions and are also only

slightly affected by trip time or propulsion time. Again, α is the significant variable (see fig. 12(b)).

As observed throughout this study, the optimum specific impulse for the electric-propulsion system, shown in figure 11(c), is almost unaffected by trip time. Furthermore, comparing figure 12(c) with figures 10(c), 8(d), 6(d), and 5(d) shows that the individual values of optimum I_{sp} are determined primarily by specific combinations of t_p and α, with little regard to mission profile or mode.

Payload Comparisons with Alternative Propulsion Systems

This section contrasts the nuclear-electric spacecraft mission results with those of other propulsion system types to indicate their relative levels of performance in terms of payload capability. Payload comparisons are made between nuclear-electric, boosted-solar-electric, and all-ballistic modes for Uranus flyby and capture missions.

Flyby missions. - Figure 13 compares the performance of nuclear-electric propulsion systems (large-dashed and solid lines) with that obtainable from solar-electric (dash-dot lines) and ballistic-chemical (small-dashed lines) systems. The nuclear-electric system's operating parameters (α = 30 kg/kW and t_p = 800 days) were chosen as representative of the present input assumptions. An α of 30 kg/kW for solar-electric propulsion was chosen, both as a representative value (see ref. 3) and to facilitate a comparison of the relative effectiveness of the two electric systems. The solar-electric performance curves are based on data in reference 4, suitably scaled up to reflect the use of the Titan IIID(7)/Centaur launch vehicle. Solar-electric propulsion time is not limited for these cases but is effectively held to 1000 to 1200 days by the falloff of solar power during the mission. The ballistic system performance curves are taken from the appendix. The appendix contains a brief analysis of payload capability for all-ballistic versions of missions to Uranus. Examples given in the appendix for a Saturn V/Centaur ballistic system are not included in these comparisons.

Consider first the two upper curves in figure 13. Clearly, the initial-spiral nuclear-electric system gives comparable performance to the large SIC/SIVB-based ballistic systems, which require not only a Centaur but also a VUS[1] upper stage. The use of nuclear-electric propulsion would bring about a substantial launch-cost saving because Titan IIID(7) would be used instead of SIC/SIVB and because the need for the Centaur and the VUS would be eliminated. The savings per mission must, of course, be weighed against the development and purchase cost of a large (typically 200 kW) nuclear-electric propulsion system for the initial-spiral mode.

[1]VUS - Versatile Upper Stage - a small hydrogen-fluorine rocket now under consideration by NASA (cf. ref. 28).

Now consider the three lower curves. These yield performance comparisons among three propulsion systems, all of which are initially launched by Titan IIID(7)/Centaur. Thus, they reflect the relative propulsive effectiveness of nuclear-electric, solar-electric and chemical systems. Clearly, the nuclear-electric system outperforms the chemical by a factor of about 3 or more at all trip times. The solar-electric system performance is comparable to that of the ballistic system at short trip times (less than 2000 days), but it gradually approaches the nuclear-electric system's capability at very long trip times.[2] In any event the boosted nuclear-electric vehicle would appear to be the attractive choice in the 4-to-5 year trip-time range (e.g., 2000-kg payload at 1700 days). Here a four-to-one payload advantage over the all-ballistic Titan IIID(7)/Centaur/VUS system is obtained at the cost of providing an electric-propulsion system of about 50 kilowatts. In this trip-time range, boosted nuclear-electric spacecraft payload is comparable to that of the initial-spiral spacecraft. The initial-spiral mode yields significant payload advantages over all other systems, but only for trip times much longer than 1700 days.

Capture missions. - Figure 14 completes the payload comparisons of the nuclear-electric, solar-electric, and ballistic systems by presenting Uranus capture mission results. Again a nominal α of 30 kg/kW has been used for the electric systems. However, t_p for the nuclear-electric system has been decreased from 800 days to the more nearly optimal range of 400 to 600 days. All results are for a 2-planet-radii by 38-planet-radii, elliptical parking orbit at Uranus and, in the electric-propulsion cases, the propulsion system (including powerplant) is separated from the spacecraft prior to retrobraking the payload into elliptical orbit.

In general, all the relative payload-level comparisons in figure 14 among the nuclear-electric, solar-electric, and large and small chemical-ballistic systems are similar to those shown in figure 13 for flyby missions. The most noticeable differences are the longer trip times and the reduced payload levels. However, it can be seen in figure 14 that the ballistic results have improved relative to the electric-propulsion cases. The ballistic payloads for the SIC/SIVB/Centaur/VUS launch vehicle are clearly better than those of the nuclear-electric system for the initial-spiral mode. In addition, the results for the chemical-ballistic system based on Titan IIID strongly compete with the payload capabilities of the boosted nuclear-electric and solar-electric systems for trip times in the 2500- to 3000-day range.

---

[2]For relatively short missions, the solar-electric-propulsion trajectory must immediately head outwards toward Uranus - thus, there is an immediate dropoff in solar power available for propulsion. For very long missions, however, there is enough time for the vehicle to loop once or twice around the Sun (thus remaining longer in a region of high solar power) before beginning its final outward sweep.

Comparison with thrust-coast-thrust trajectories. - The shifts in relative performance in figure 14 are caused by the tendency of electric-propulsion trajectories toward high approach velocity relative to the target planet. Our restriction of electric propulsion to a single period is a major factor leading to high planet approach velocities. It is known that, when a second electric-propulsion period is allowed prior to planet encounter, approach velocities of electric-propulsion capture mission trajectories can be made much lower. This approach results in a thrust-coast-thrust (T-C-T) heliocentric trajectory instead of the thrust-coast (T-C) trajectory mode used throughout this study. Even with an upper limit of 600 to 800 days of total propulsion time, T-C-T trajectories could double the capture payloads of the nuclear-electric systems in figure 14.

This trend is illustrated in figure 15 where the present T-C mode is compared with the optimal T-C-T mode for boosted missions at trip times of 2500 and 3000 days. Again, α is 30 kg/kW. Payload is plotted against total propulsion time; and it is quite evident that, except at very low t_p's, the T-C-T mode outperforms the present one by a factor of about 2. On the other hand, T-C-T trajectories require electric-propulsion systems which are restartable after long coast periods (e.g., 3 to 6 years). Their significant payload advantages are achieved for total propulsion times usually exceeding 800 days and require that the propulsion system be available during the whole mission duration of 6 to 8 years. Demonstration and qualification for such lifetime requirements would introduce major delays in the development process of the propulsion system.

Perturbations in propulsion time and specific powerplant mass. - Since propulsion system lifetime and α are not well-established, it is fitting to discuss the effects of changes in these parameters on the comparisons in figures 13 and 14. In the flyby missions of figure 13, reducing propulsion system lifetime below 800 days would decrease the payload of the boosted nuclear-electric spacecraft by no more than 4 percent for each 100-day decrease in t_p, based on figures 5(a) and 6(a). Initial-spiral-mode flyby missions are more sensitive to changes in t_p, but the payload decrease is only about 8 percent per 100-day decrease in t_p, as indicated in figure 10(a). The capture mission results in figure 14 have a similar or lesser sensitivity to changes in t_p since the t_p's of 600 days and 400 days used for the initial-spiral and boosted modes, respectively, are near optimum, as can be seen in figures 8(a) and 12(a).

As noted earlier, nuclear-electric spacecraft payloads, for the ranges of T, t_p, and α of this study, are more sensitive to variations in α than in t_p. The sensitivity to α is about the same in both boosted and initial-spiral mission modes. Because of the added features of propulsion system jettison and retrorocket requirements in capture missions, the effects of α variations are more easily seen in flyby mission results. Referring back to figures 5(a), 6(a), and 10(a), a change in α of 10 kg/kW, when α initially equals 30 kg/kW, changes the flyby payload by an amount equal to about 12 percent of the spacecraft total mass. For initial-spiral missions, 12 percent of the initial mass is

about 2000 kilograms. For boosted flyby missions, since initial mass varies, the 12-percent payload change for a 10-kg/kW change in α is 500 to 700 kilograms.

Spacecraft Design Characteristics

Table I contains selected examples of trajectory and spacecraft characteristics for boosted and initial-spiral mission modes. By reviewing table I and other results and comparisons made in this study, certain general design considerations for the electric-propulsion spacecraft can be observed.

Travel time. - The duration of each mission sets the lifetime requirements for the spacecraft payload and support subsystems. For missions beyond Jupiter, it appears that travel times must be 3 or more years. The Uranus flyby trip times of 1500 days (4 yr) and capture mission trip times of 2500 days (7 yr) given in table I are somewhat short, representing the lower ranges of payload capability. Data discussed in an earlier subsection of this report show that each additional 100 days travel time allows a 100- to 200-kilogram increase in payload. However, such gains in payload must be weighed against the possible penalties of longer required operating life for the payload systems.

Propulsion time. - The single-burn propulsion time of each case in table I is given in the extreme right-hand column. The results of this study have indicated that a single propulsion period of 400 to 800 days is sufficient for most missions. For capture missions, propulsion time can optimize in the range of 400 to 600 days. However, payload penalties become severe in most cases as t_p is reduced below 400 days.

Although this study emphasizes single-burn electric propulsion, it is noted that a restartable propulsion system (cf. fig. 15) needs only 800 to 1200 days of total propulsion time to achieve most of its payload potential. However, for these systems, the propulsion time must be interrupted by a coast period of up to 6 years.

Specific impulse. - Optimum specific-impulse values range from 3000 to 8000 seconds, mostly because of the effects of varying t_p and α. For fixed combinations of t_p and α, optimum I_{sp} is relatively unaffected by travel time or mission mode. As noted earlier in this study, optimum I_{sp} can be closely approximated by a simple function of $\sqrt{t_p/\alpha}$. Table I shows that the optimum I_{sp} for initial-spiral missions is usually about 20 percent less than that for boosted missions when t_p and α are the same.

Planet approach velocity. - Unlike flybys, optimum trajectories for capture missions are compromised to decrease the planet approach velocity, thereby reducing the braking-rocket-system mass requirement. The decrease in approach velocity between the boosted 2500-day flyby and capture missions can be compared in table I. The penalty for this velocity reduction is a decrease in the mass delivered to planet encounter. For example, the combined mass of the braking rocket system and the payload for the 2500-day

capture mission is 100 to 500 kilograms less than the allowable payload of an equivalent 2500-day flyby mission. Table I also shows, for each α, the increase in approach velocity with increased t_p, which causes t_p to optimize at low values in capture missions.

Typical boosted spacecraft. - The comparisons made in this study indicate that, for the same basic launch vehicle, electric-propulsion spacecraft payload capability in the boosted mission mode is generally less than that of the initial-spiral mode. It was noted, however, that boosted missions may be desirable since payloads far greater than one-half of the initial-spiral capability are achieved with boosted spacecraft having far smaller total mass and installed power. Furthermore, boosted-mode payloads can be greater than initial-spiral payloads at very short trip times, subject, of course, to the effects of allowable t_p and α.

A nominal boosted-mode spacecraft for the Titan IIID(7)/Centaur launch vehicle would have a total mass between 5000 and 7000 kilograms, because of mission-dependent variations in launch velocity. Propulsion system and propellant mass fractions for a relatively short trip time would be about 33 percent each, leaving a flyby payload capability of about 33 percent of the total mass, or 1600 to 2400 kilograms. As stated earlier, installed power level would vary more widely, as α changes, than would the mass of the propulsion system. Optimum power level could range from 40 kilowatts, for an α of 40 kg/kW, to as high as 100 kilowatts for an α of 20 kg/kW.

For Uranus capture missions, 70 to 80 percent of the spacecraft mass at the orbit insertion point must be allocated to the chemical rocket braking system. Hence, capture mission payloads would range from 400 to 600 kilograms unless longer trip times were allowed.

Typical initial-spiral spacecraft. - The present study indicates that, except for very short trip times, the initial-spiral mode yields the highest payload potential for electric-propulsion spacecraft. Spacecraft for this mode generally require larger propellant fractions than boosted spacecraft, reflecting the extra propulsion requirement of escaping the Earth under their own power. The escape spiral time represents about one-third of the total allowed propulsion time and one-third of the propellant used in a typical mission.

A typical spacecraft for the initial-spiral mode at short trip times would be apportioned into 35 percent for the propulsion system and 50 percent for the propellant and tankage, leaving about 15 percent for flyby payload. However, at very short trip times (such as 1600 days), the flyby payload fraction can drop to 10 percent because of increased power and propellant requirements. For the Titan IIID(7) launch vehicle assumed in this study, total mass of the initial-spiral spacecraft is 17 300 kilograms. Therefore, the masses of the propulsion system, propellant, and flyby payload would be about 6000, 8500, and 2500 kilograms, respectively. Optimum power levels would range from 150 to 300 kilowatts, depending primarily on α.

As in boosted-mode spacecraft, a chemical-propulsion braking rocket system would be required if capture in Uranus orbit were desired. In such a case the 2500-kilogram flyby payload would be divided into 500 to 800 kilograms for captured payload and 1700 to 2000 kilograms for the braking rocket. Again, as in the boosted mode, increasing allowed trip time significantly increases payload capability.

CONCLUDING REMARKS

This report has evaluated the performance of a single-propulsion-period concept for nuclear-electric spacecraft on missions to Uranus. This mode of operation is suitable for first-generation-type nuclear-electric power systems since the total useful lifetime need not extend beyond the first 400 to 800 days of the mission. The spacecraft can be launched by a Titan IIID(7) or the Space Shuttle having similar launch performance. Total spacecraft mass and electric power level are 17 000 kilograms and about 150 to 300 kilowatts for electric-propulsion systems intended to escape from low Earth orbit under their own power on a low-thrust spiral trajectory. Alternatively, if the electric spacecraft is boosted to Earth escape by a Centaur launch vehicle, the total mass and power requirements are 5000 to 7000 kilograms and 40 to 100 kilowatts, respectively.

Even with the constraints imposed on the nuclear-electric systems in this study, they show substantial payload advantages over ballistic mission systems based on the same launch vehicle, except at extremely short trip times, where payloads of all systems are negligible. The only significant gains in ballistic-mode performance are achieved by employing a much larger launch vehicle system.

The single-thrust-period propulsion profile for nuclear-electric systems yields payload performance less than that of the more optimum, but more complex, thrust-coast-thrust operation. However, performance is comparable at low values (10 000 hr) of allowed propulsion time. Hence, the development of systems which are restartable after long "off," or coast, periods, such as 3 to 5 years, may be deferred while useful applications of simpler thrust-coast systems are inaugurated at an earlier date and, probably, at a lower cost.

Lewis Research Center,
National Aeronautics and Space Administration,
Cleveland, Ohio, October 2, 1972,
501-04.

APPENDIX - BALLISTIC MISSIONS TO URANUS

This appendix develops ballistic-mission payload estimates for Uranus flyby and capture for the purpose of comparison with systems employing nuclear-electric propulsion. The ballistic missions are based on three advanced launch vehicles whose launch capabilities are illustrated in figure 16. The figure shows injected mass capability (launch vehicle payload) at injection velocities above Earth escape speed.

The lowest curve in figure 16 is for the basic launch vehicle of this study, the Titan IIID(7), whose performance is augmented by the addition of both the Centaur and an advanced chemical-propulsion upper stage called the VUS. This is a newly proposed versatile upper stage, discussed in reference 28, with performance and characteristics that are not firmly established. The highest curve in the figure is for the Saturn V launch vehicle with the Centaur added as an upper stage to increase injection mass capability for injection velocities far above Earth escape speed. The middle curve in figure 16 shows the injected mass capability of the SIC/SIVB/Centaur/VUS launch vehicle system. This launch vehicle is typical of so-called intermediate launch vehicle systems intended to fill the gap in payload and cost between the Titan III-based systems and the Saturn V.

Launch vehicle capability displayed in figure 16 is translated into ballistic-mission payload capability by the velocity requirements given in figure 17. There, required launch velocity at Earth and approach velocity at Uranus arrival are given for a range of Earth-Uranus trip times. The velocities in this figure apply only to ballistic missions and are based on the same circular-coplanar heliocentric orbits for Earth and Uranus assumed throughout this study.

In figure 17, the curve of required launch velocity at low Earth altitude is derived from the necessary hyperbolic departure velocities for ballistic trajectories to Uranus at each trip time. The launch velocities on this curve correspond directly to the launch velocity scale shown in figure 16. Launch vehicle payloads for all-ballistic Uranus flyby missions are read from figure 16 at the appropriate launch velocity given in figure 17 for each trip time.

The Uranus encounter curve in figure 17 (dashed line) gives the velocity of the ballistic spacecraft relative to Uranus upon arrival. This velocity is needed to calculate retrorocket propellant requirements for all-ballistic capture missions. Both Uranus velocity curves minimize at a trip time of about 5850 days, which is the Hohmann or minimum-energy case for ballistic trajectories to Uranus. Except for differences in trip time, similar velocity ranges would be covered by each curve for ballistic trajectories to all four major planets: Jupiter, Saturn, Uranus, and Neptune. For example, the other curves given in figure 17 show that the minimum launch velocity at Earth for Earth-to-Jupiter ballistic mission trajectories is about 14.1 km/sec and that the minimum relative approach velocity to Jupiter is 5.6 km/sec. But the Hohmann trip time to Jupiter is 1000 days, instead of the nearly 6000 days required for Uranus.

Payloads for ballistic missions to Uranus are given in figure 18. Data are shown for both flyby and capture missions based on the three different launch vehicles: Saturn V/Centaur, SIC/SIVB/Centaur/VUS, and the Titan IIID(7)/Centaur/VUS. The choice of capture parking orbit (2×38 ellipse) and the parameters assumed for the braking rocket system are the same as used throughout this report for the electric-propulsion missions.

Trip times to Uranus above 4000 days are not shown in figure 18. As suggested by the flattening of the curves shown in the figure, there is very little payload increase above 4000 days although, as noted in figure 17, the Hohmann ballistic trajectory requires a trip time of more than 5800 days.

REFERENCES

1. Kerslake, W. R.; Goldman, R. G.; and Nieberding, W. C.: Sert II: Mission, Thruster Performance, and In-Flight Thrust Measurements. J. Spacecraft Rockets, vol. 8, no. 3, Mar. 1971, pp. 213-224.

2. Kerslake, William R.; and Reader, Paul D.: Kaufman Thruster Development at Lewis Research Center. NASA TM X-67915, 1971.

3. Willis, E. A., Jr.; Hrach, F. J.; Strack, W. C.; and Zola, C. L.: Prospects for a Multipurpose Solar Electric Propulsion Stage. NASA TM X-67801, 1971.

4. Zola, Charles L.: Interplanetary Probe Missions with Solar-Electric Propulsion Systems. NASA TN D-5293, 1969.

5. Anon.: Study of a Common Solar-Electric-Propulsion Upper Stage for High-Energy Unmanned Missions. Vol. 1: Summary. Rep. TRW-16552-6006-RO-OO-Vol. -1, TRW Systems Group (NASA CR-114349), July 14, 1971.

6. Anon.: Study of a Common Solar-Electric-Propulsion Upper Stage for High-Energy Unmanned Missions. Vol. 2: Technical. Rep. TRW-16552-6007-RO-OO-Vol. -2, TRW Systems Group (NASA CR-114350), July 14, 1971.

7. Anon.: Study of a Common Solar-Electric-Propulsion Upper Stage for High-Energy Unmanned Missions. Vol. 3: Appendixes. Rep. TRW-16552-6008-RO-OO-Vol. -3, TRW Systems Group (NASA CR-114351), July 14, 1971.

8. Spencer, Dwain F.; Jaffe, Leonard D.; Lucas, John W.; Merrill, Owen S.; and Shafer, John I.: Nuclear Electric Spacecraft for Unmanned Planetary and Interplanetary Missions. Electric Propulsion Development. Vol. 9 of Progress in Astronautics and Aeronautics. Ernst Stuhlinger, ed., Academic Press, 1963, pp. 665-685.

9. Beale, Robert J.: Nuclear-Electric Spacecraft Concepts for Unmanned Planetary Exploration. IRE Trans. on Space Electronics and Telemetry, vol. SET-8, no. 2, June 1962, pp. 178-182.

10. Larson, J. W.: Research on Spacecraft and Powerplant Integration Problems. Rep. 64SD892, General Electric Co. (NASA CR-54159), July 24, 1964.

11. Anon.: Navigator Study of Electric Propulsion for Unmanned Scientific Missions. Rep. 65SD4298, General Electric Co. (NASA CR-54349), July 15, 1965.

12. Fimple, W. R.: Application of Electric Propulsion for Selected Unmanned NASA Space Missions. Rep. C-910076-4, United Aircraft Corp. (NASA CR-58891), Sept. 1964.

13. Anon.: Electrical Power Generation Systems for Space Applications. NASA SP-79, 1965.

14. Anon.: Space Power Systems Advanced Technology Conference. NASA SP-131, 1966.

15. Ragsac, R. V.: Study of Low-Acceleration Space Transportation Systems. Vol. 1: Summary Report. Rep. F-910262-20, Vol. 1, United Aircraft Corp. (NASA CR-90554), Oct. 1967.

16. Ragsac, R. V.: Study of Low-Acceleration Space Transportation Systems. Vol. 2: Technical Report. Rep. F-910262-20, Vol. 2, United Aircraft Corp. (NASA CR-90553), Oct. 1967.

17. Ragsac, R. V.: Study of Low-Acceleration Space Transportation Systems. Vol. 3: Low-Acceleration Interplanetary Flight Handbook. Rep. F-910262-20, Vol. 3, United Aircraft Corp. (NASA CR-90556), Oct. 1967.

18. Pitts, John H.; and Walter, Carl E.: Conceptual Design of a 10-MWe Nuclear Rankine System for Space Power. J. Spacecraft Rockets, vol. 7, no. 3, Mar. 1970, pp. 259-265.

19. Pitts, John H.; and Walter, Carl E.: Conceptual Design of a 2-MWt (375 kWe) Nuclear-Electric Space Power System. J. Spacecraft Rockets, vol. 7, no. 11, Nov. 1970, pp. 1282-1286.

20. Breitwieser, Roland; and Lantz, Edward: A Design Study of a 350 kWe Out-of-Core Nuclear Thermionic Converter System. NASA TN X-52846, 1970.

21. Ward, James J.; Breitwieser, Roland, and Williams, Richard M.: Conceptual Design of a 150 kWe Out-of-Core Nuclear Thermionic Converter System. Proceedings of the Ninth Thermionic Conversion Specialist Conference. IEEE, 1970, pp. 179-184.

22. Mondt, J. F.; and Davis, J. P.: Thermionic Reactor Electric Propulsion Spacecraft for Unmanned Outer Planet Exploration. Paper 70-1122, AIAA, Sept. 1970.

23. Boman, L. H.; and Gallagher, J. G.: NERVA Technology Reactor Integrated with NASA Lewis Brayton Cycle Space Power Systems. J. Spacecraft Rockets, vol. 8, no. 5, May 1971, pp. 500-505.

24. Kerwin, Paul T.: Design Point Characteristics of a 15-to-80 kWe Nuclear-Reactor Brayton-Cycle Power System. Proceedings of the Intersociety Energy Conversion Engineering Conference. SAE, 1971, pp. 376-381.

25. Klann, John L.; and Wintucky, William T.: Status of the 2-to-15 kWe Brayton Power System and Potential Gains from Component Improvements. Proceedings of the Intersociety Energy Conversion Engineering Conference. SAE, 1971, pp. 195-201.

26. Strack, William C.; and Huff, Vearl N.: The N-Body Code - A General FORTRAN Code for the Numerical Solution of Space Mechanics Problems on an IBM 7090 Computer. NASA TN D-1730, 1963.

27. Kendrick, J. B., ed.: TRW Space Data. TRW Systems Group, 1967.

28. Anon.: Launch Vehicle Estimating Factors. NASA Office of Space Science and Applications, Launch Vehicle, and Propulsion Programs, Jan. 1971.

29. Anon.: Space Shuttle Baseline Accommodations for Payloads. MSC-06900 Payload Engineering Office, Future Programs Division, Engineering and Development Directorate, Manned Spacecraft Center, Houston, Tex., June 1972.

30. Anon.: Compatibility of a Cryogenic Upper Stage With Space Shuttle. Rep. GDCA-BNZ71-020-7 General Dynamics/Convair (NASA CR-120897), Apr. 1972.

31. Moeckel, W. E.: Propulsion Systems for Manned Exploration of the Solar System. NASA TM X-1864, 1969.

TABLE I. - SUMMARY OF SYSTEMS FOR FLYBY AND ELLIPTICAL CAPTURE MISSIONS TO URANUS

Mission mode		Trajectory				Mass allocation, kg					Propulsion system				
		Total travel time, days	Escape spiral time, days	Launch velocity at Earth (185-km altitude), km/sec	Planet approach velocity, km/sec	Initial mass	Powerplant power conditioner thrusters	Propellant and tankage	Braking rocket system	Gross payload	Power, kW	Specific impulse, I, sec	Overall efficiency, η	Powerplant specific mass, α, kg/kW	Propulsion time, t_p, days
Flyby	Boosted	1500	---	11.48	22.61	6 300	1920	2 240	----	2140	96	5150	0.775	20	400
			---	11.41	27.20	6 450	1860	2 270	----	2320	93	7250	.811	20	800
			---	12.27	22.01	4 680	1560	1 700	----	1420	52	4255	.745	30	400
			---	12.06	26.04	5 070	1590	1 880	----	1600	53	5964	.793	30	800
	Initial spiral	1500	126	7.8	24.56	17 300	5900	9 390	----	2010	295	4290	0.746	20	400
			192	↓	30.83	↓	5520	8 650	----	3130	276	6300	.800	20	800
			137	↓	24.80	↓	6400	11 500	----	----	214	3160	.676	30	400
			205	↓	31.65	↓	6000	10 660	----	640	200	4750	.763	30	800
	Boosted	2500	---	11.17	11.57	7 050	1800	1 900	----	3260	90	5295	0.779	20	400
			---	11.03	14.04	7 400	1660	2 020	----	3720	83	7319	.811	20	800
			---	11.52	11.38	6 250	1800	1 950	----	2500	60	4377	.750	30	400
			---	11.08	14.04	7 300	1860	2 500	----	2940	62	5875	.791	30	800
Capture	Boosted	2500	---	11.48	11.25	6 300	1540	1 600	2260	900	77	5450	0.783	20	400
			---	11.64	11.65	5 930	1360	1 400	2340	830	68	6800	.805	20	600
			---	11.92	11.11	5 340	1260	1 630	1730	720	42	4600	.745	30	400
			---	12.18	11.47	4 830	1110	1 260	1800	660	37	5550	.785	30	600
	Initial spiral	2500	154	7.8	12.07	17 300	5250	7 200	3700	1150	263	4700	0.762	20	400
			205	↓	12.93	↓	4830	6 590	4770	1110	242	5880	.791	20	600
			160	↓	12.11	↓	6110	8 700	1910	580	204	3640	.713	30	400
			214	↓	13.08	↓	5580	7 850	3170	700	186	4610	.759	30	600

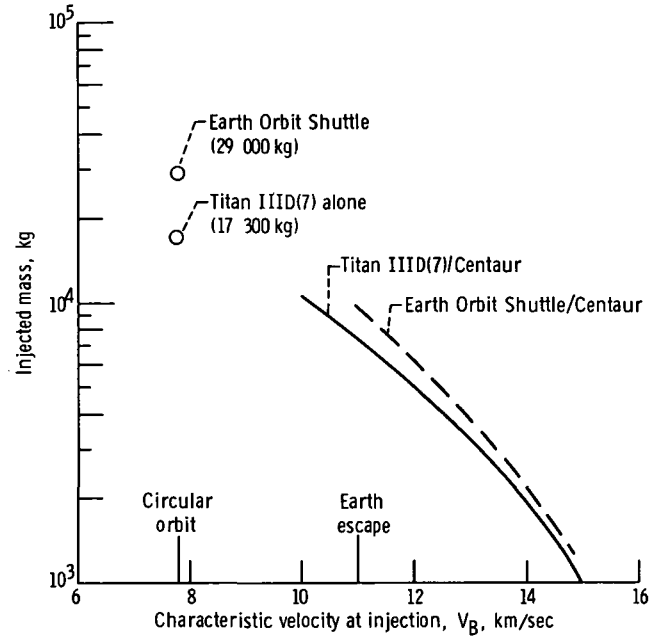

Figure 1. - Injected mass capability of launch vehicles based on the Titan IIID(7) or Earth Orbit Shuttle to various velocities at 185-kilometer altitude for due-East launches from Eastern Test Range.

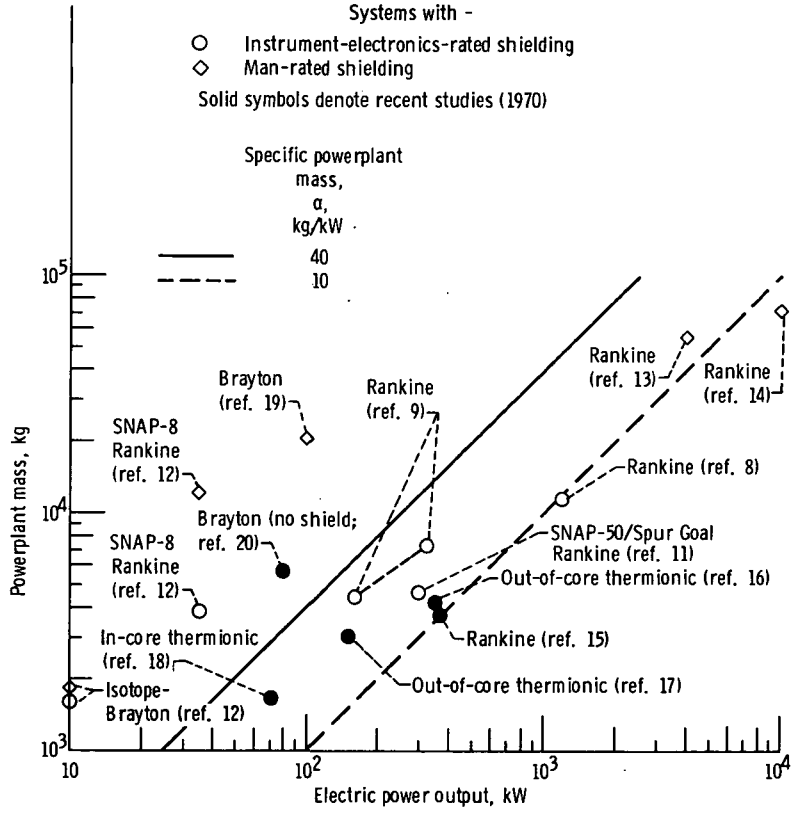

Figure 2. - Mass of various nuclear-electric space powerplants.

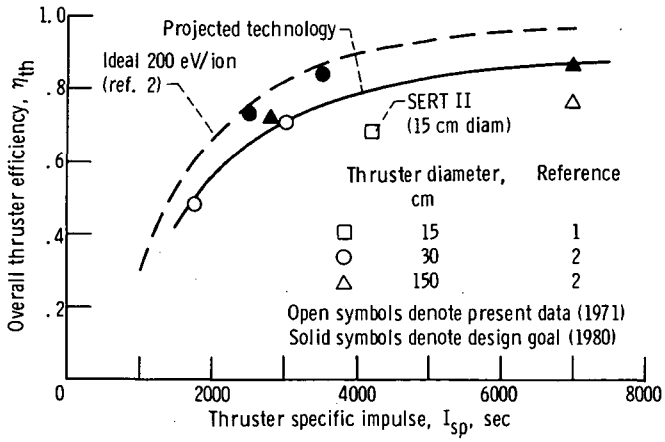

Figure 3. - Mercury-ion (Kaufman) thruster efficiency.

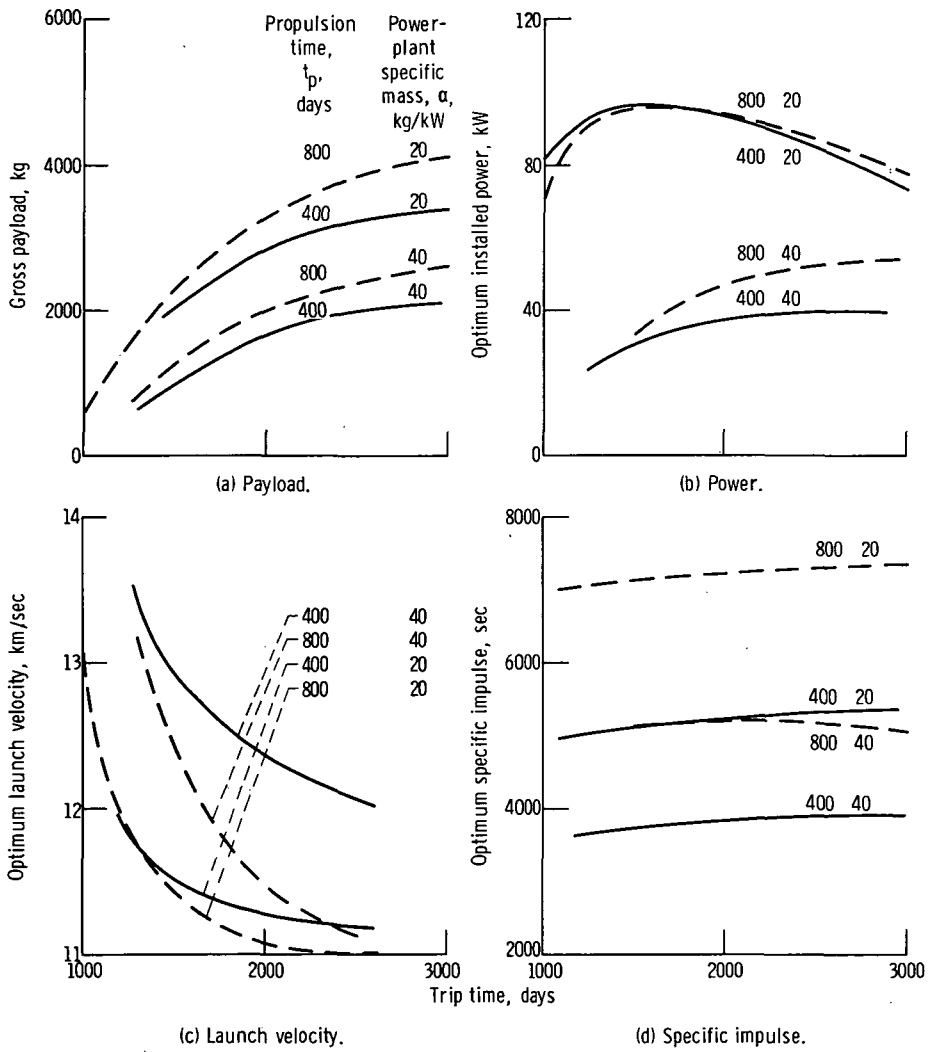

Figure 4. - Uranus flyby using boosted mission mode, showing effect of trip time on optimum specific impulse, installed power, launch velocity, and gross payload. Nuclear-electric spacecraft launched to Earth escape speed or greater by Titan IIID(7)/Centaur launch vehicle.

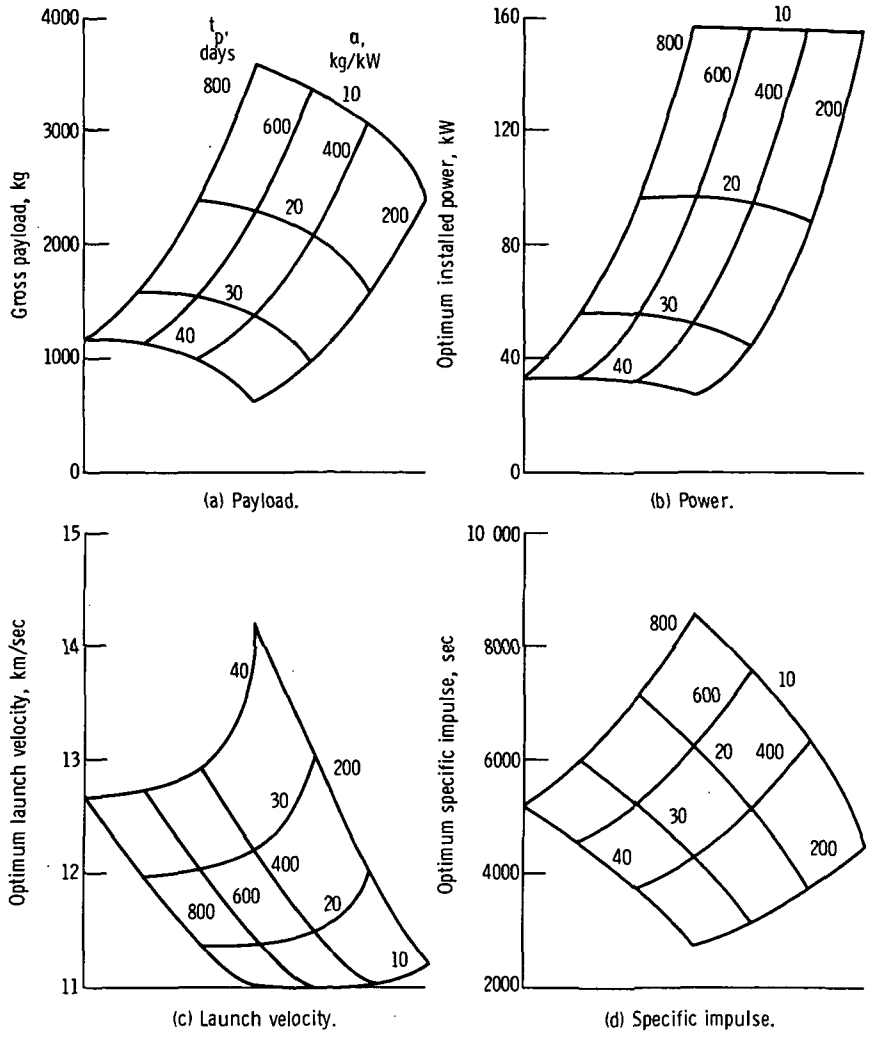

Figure 5. - Uranus flyby using boosted mission mode, for trip time of 1500 days. Effect of propulsion time t_p and specific powerplant mass α on optimum specific impulse, installed power, launch velocity, and gross payload. Nuclear-electric spacecraft launched to Earth escape speed or greater by Titan IIID(7)/Centaur launch vehicle.

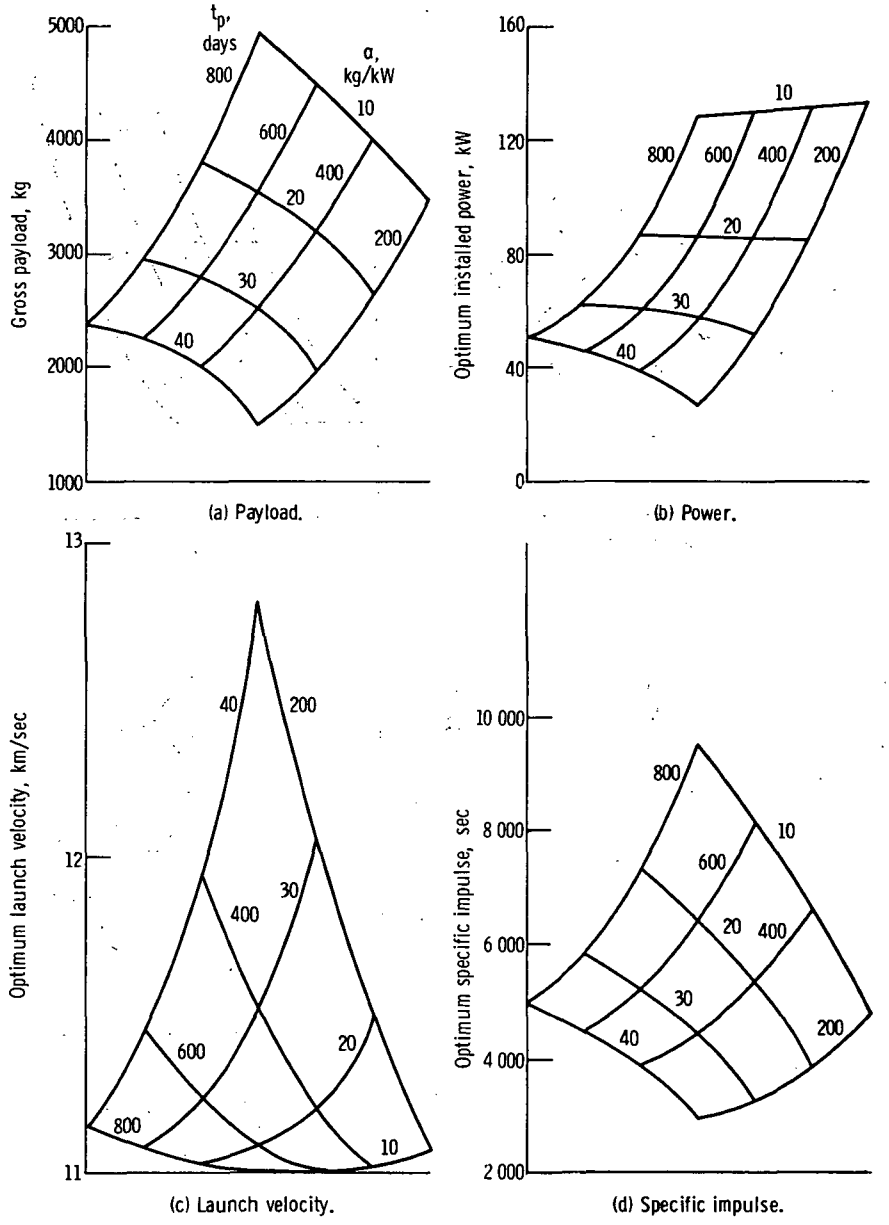

Figure 6. - Uranus flyby using boosted mission mode, for trip time of 2500 days. Effect of propulsion time t_p and specific powerplant mass α on optimum specific impulse, installed power, launch velocity, and gross payload. Nuclear-electric spacecraft launched to Earth escape speed or greater by Titan IIID(7)/Centaur launch vehicle.

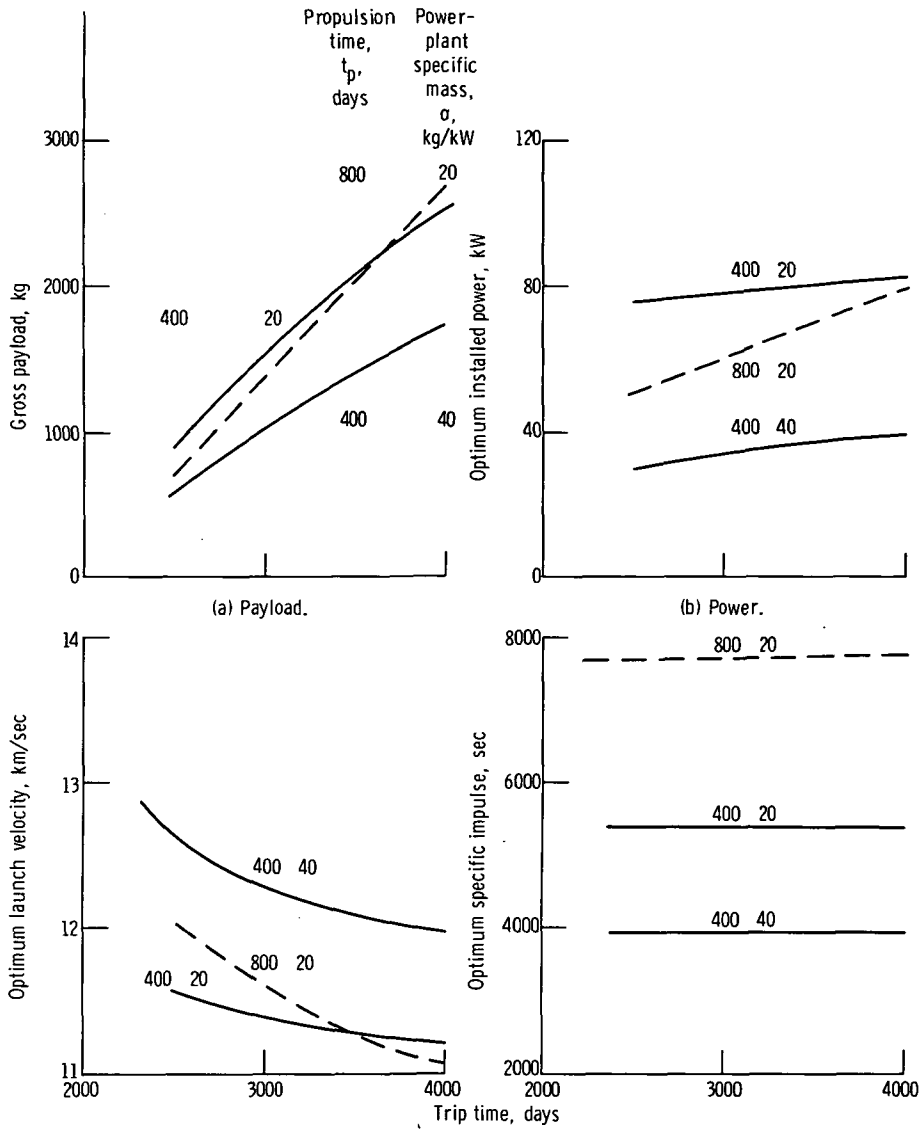

Figure 7. - Uranus flyby using boosted mission mode, showing effect of trip time on optimum specific impulse, installed power, launch velocity, and gross payload. Nuclear-electric spacecraft launched to Earth escape speed or greater by Titan IIID(7)/Centaur launch vehicle. High-thrust retrobraking into 2x38 elliptical parking orbit at Uranus.

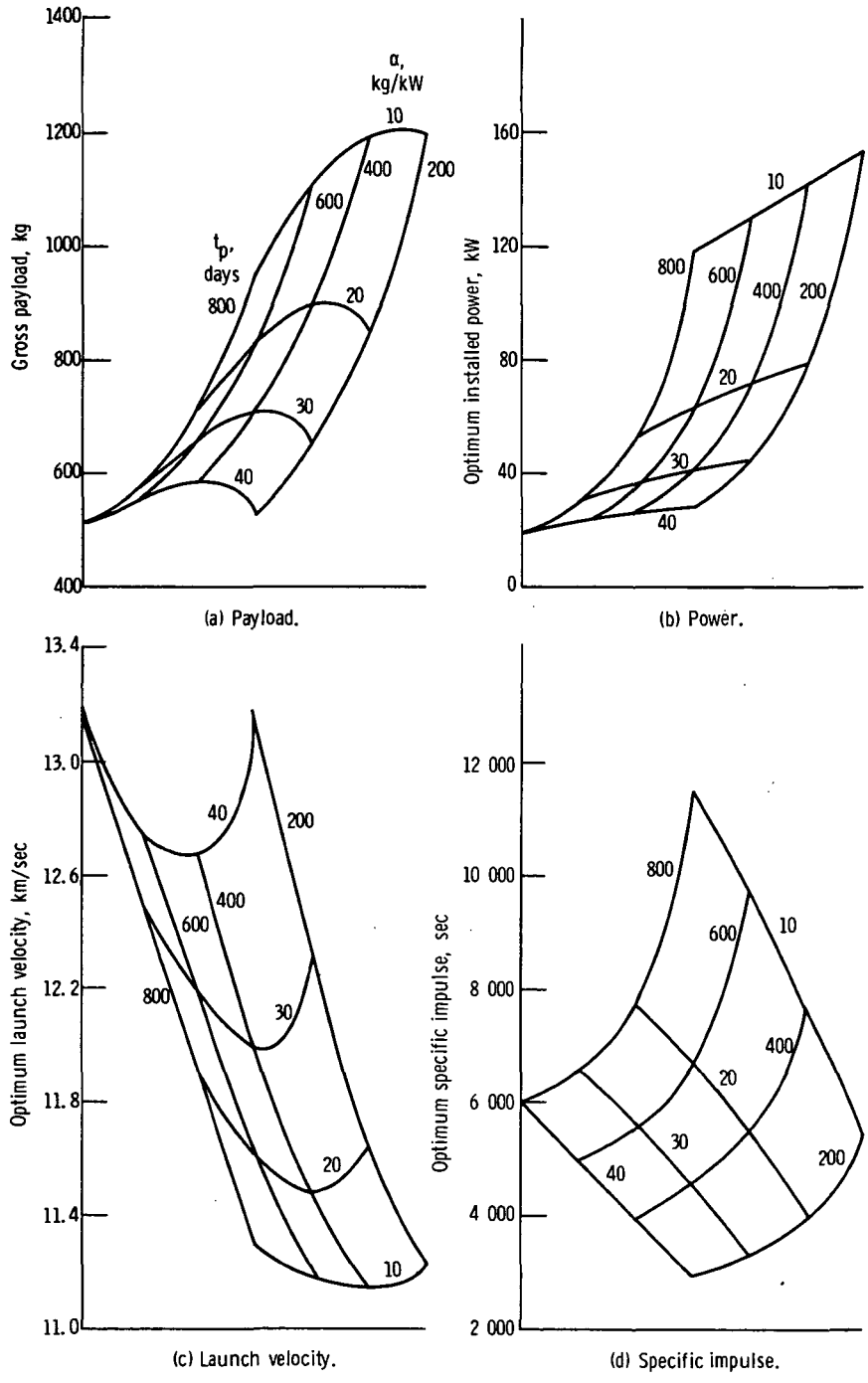

Figure 8. - Uranus capture using boosted mission mode, for trip time of 2500 days. Effect of propulsion time t_p and specific powerplant mass α on optimum specific impulse, installed power, launch velocity, and gross payload. Nuclear-electric spacecraft launched to Earth escape speed or greater by Titan IIID(7)/Centaur launch vehicle. High-thrust retrobraking into 2x38 elliptical parking orbit at Uranus.

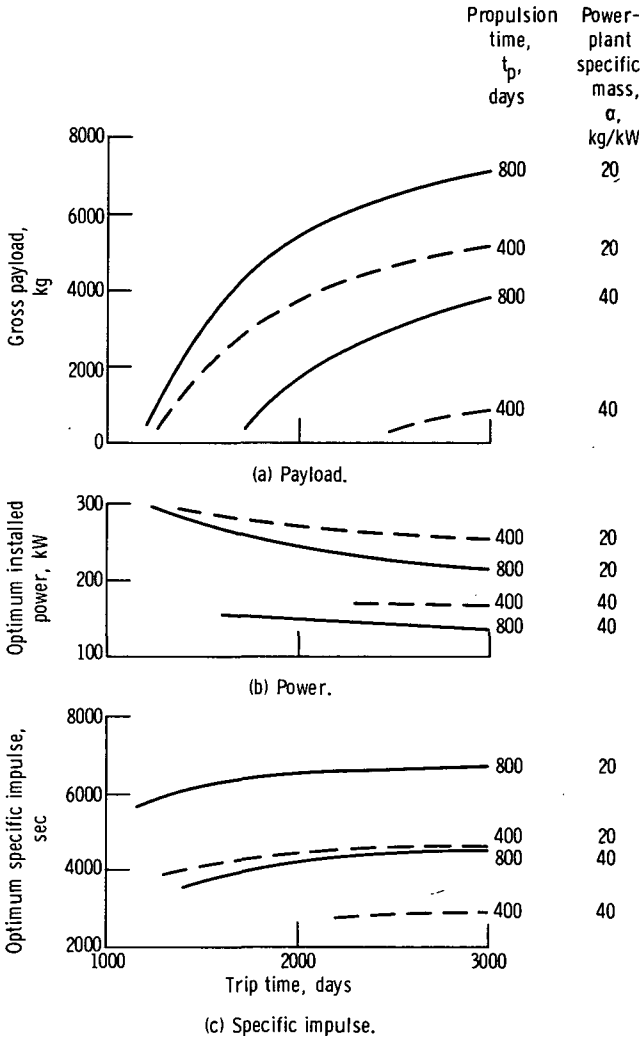

Figure 9. - Uranus flyby using initial-spiral mode, showing effect of trip time on optimum specific impulse, installed power, and gross payload. Nuclear-electric spacecraft launched to low Earth orbit by Titan IIID(7) launch vehicle.

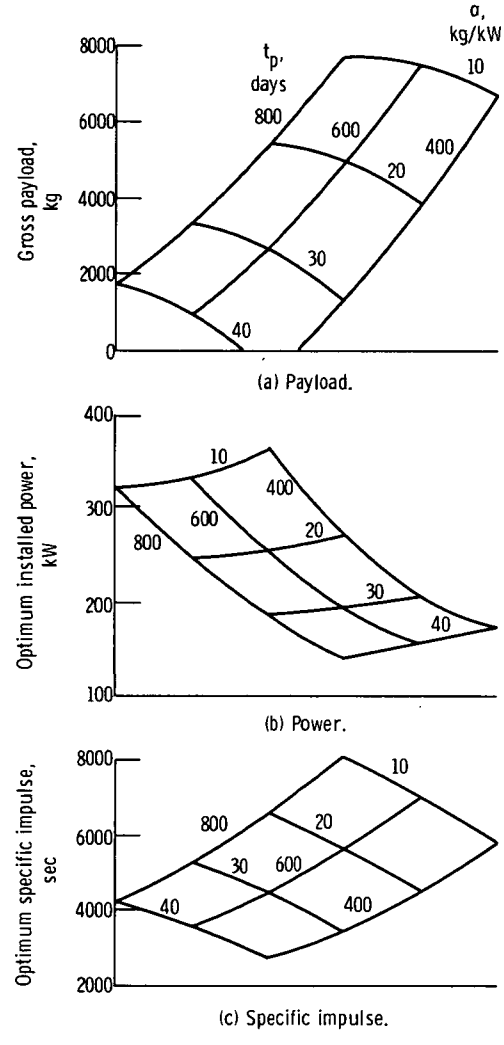

Figure 10. - Uranus flyby using initial-spiral mode, for trip time of 2000 days. Effect of propulsion time t_p and specific powerplant mass α on optimum specific impulse, installed power, and gross payload. Nuclear-electric spacecraft launched to low Earth orbit by Titan IIID(7) launch vehicle.

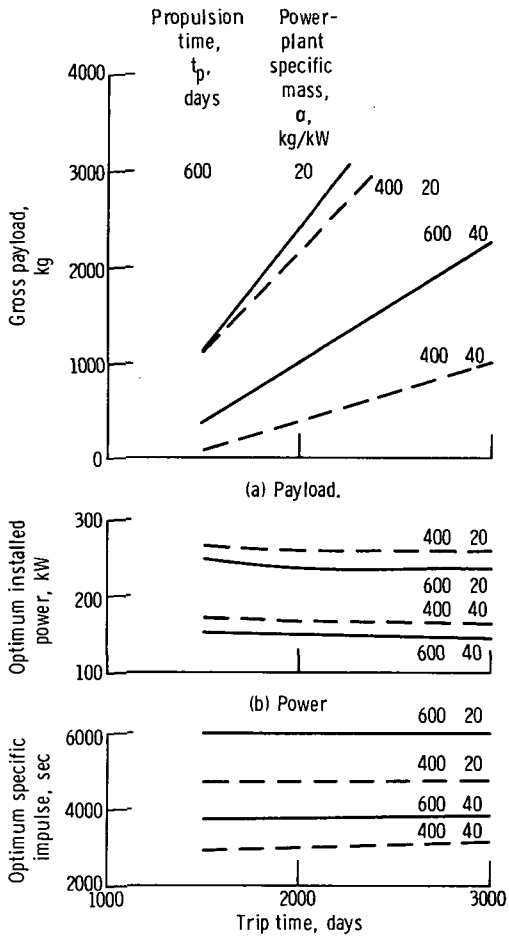

Figure 11. - Uranus capture using initial-spiral mode, showing effect of trip time on optimum specific impulse, installed power, and gross payload. Nuclear-electric spacecraft launched to low Earth orbit by Titan IIID(7) launch vehicle. High-thrust retrobraking into 2x38 elliptical parking orbit at Uranus.

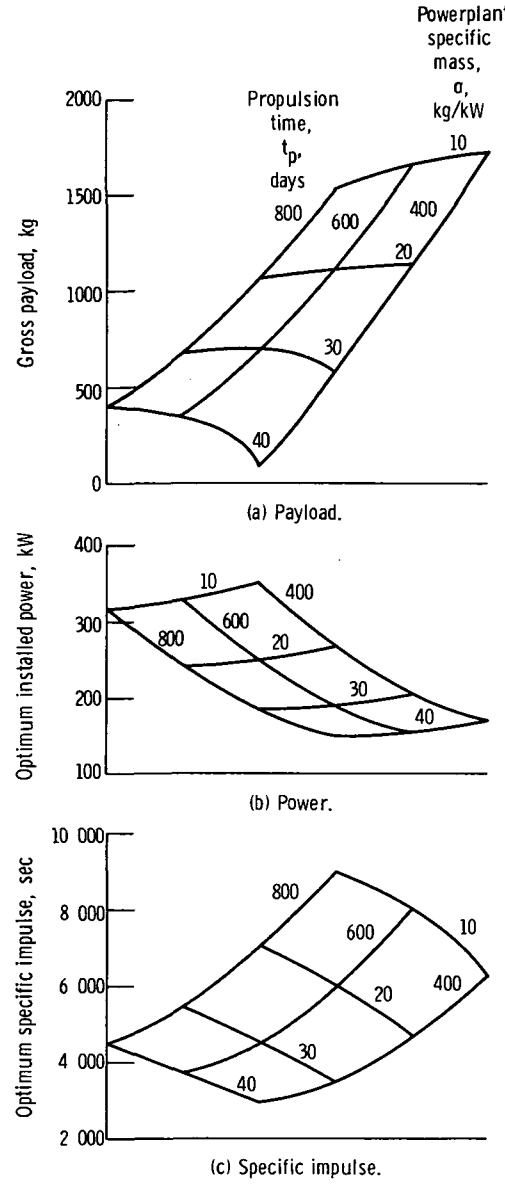

Figure 12. - Uranus capture using initial-spiral mode, for trip time of 2500 days. Effect of propulsion time t_p and specific powerplant mass α on optimum specific impulse, installed power, and gross payload. Nuclear-electric spacecraft launched to low Earth orbit by Titan IIID(7) launch vehicle. High-thrust retrobraking into 2x38 elliptical parking orbit at Uranus.

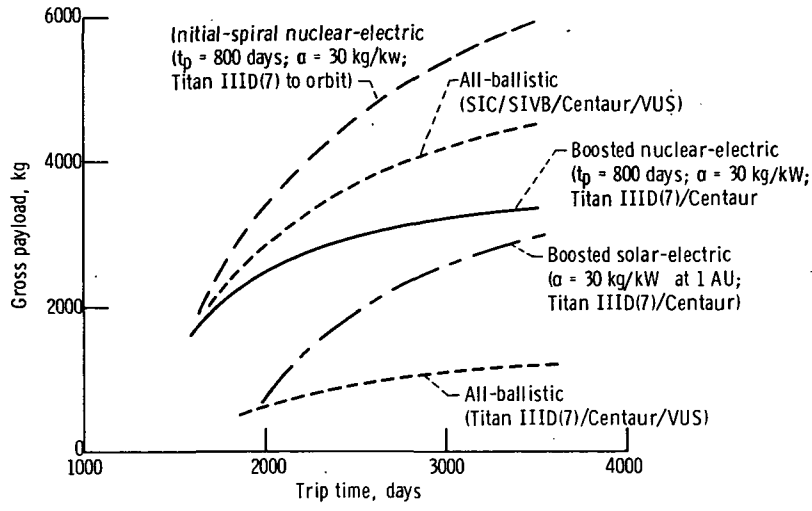

Figure 13. - Uranus flyby mission - comparison of nuclear-electric, solar-electric, and ballistic mission modes.

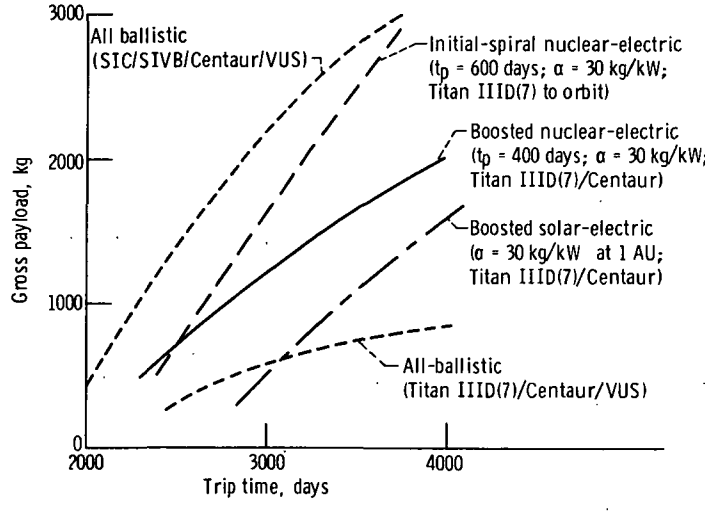

Figure 14. - Uranus capture mission - comparison of nuclear-electric, solar-electric, and all-ballistic mission modes. All cases include chemical rocket retrobraking into 2x38 elliptical parking orbit at Uranus.

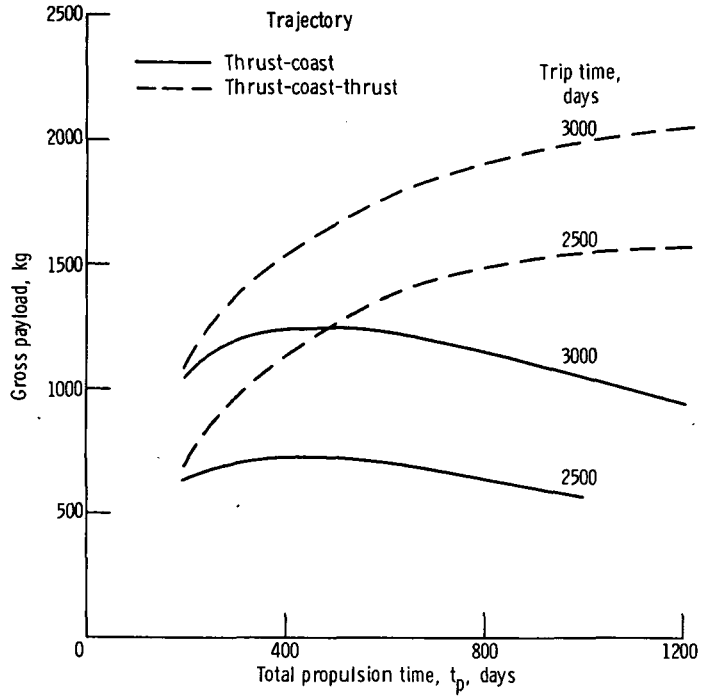

Figure 15. - Comparison of optimum thrust-coast-thrust and thrust-coast trajectories for Uranus capture missions. Titan IIID(7)/Centaur launch vehicle; powerplant specific mass, 30 kg/kW; high-thrust retrobraking into 2x38 elliptical parking orbit at Uranus in all cases.

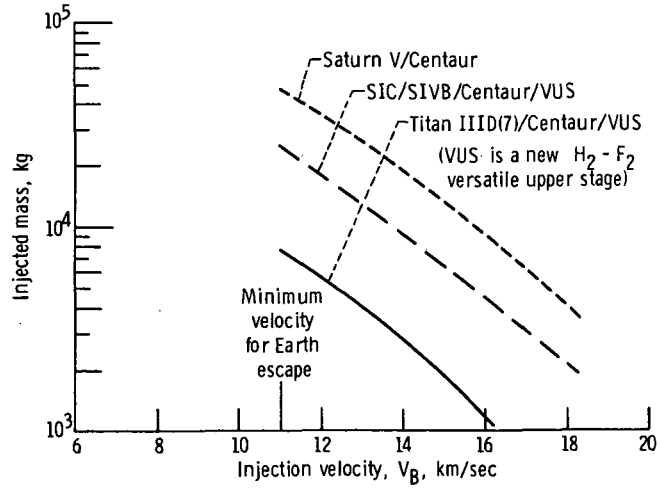

Figure 16. - Injected (or launch) mass capability of various launch vehicles for Earth escape from low altitude (185 km). Due-East launch from Eastern Test Range.

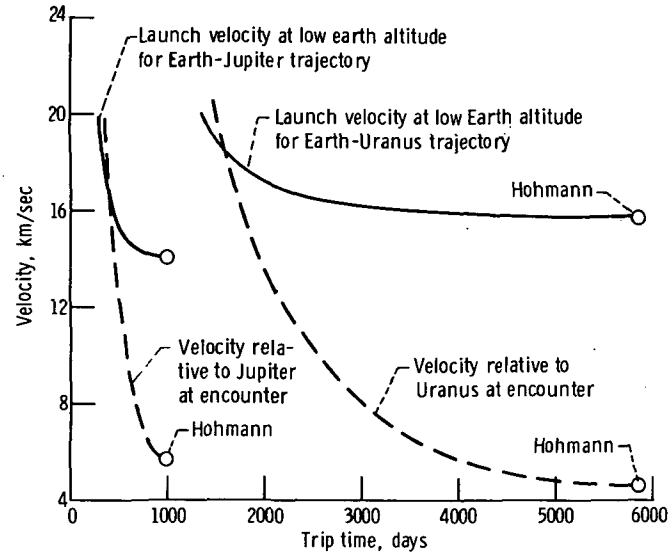

Figure 17. - Velocities for flyby and capture ballistic missions to Uranus and Jupiter.

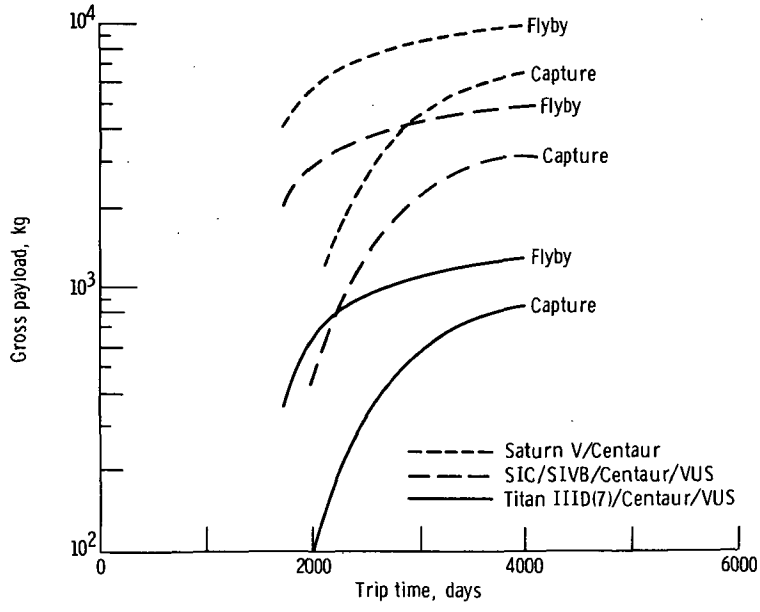

Figure 18. - Gross payloads for flyby and capture ballistic missions to Uranus for three launch vehicle systems. Chemical braking (I = 420 sec) into 2x38 elliptical capture orbit; retropropulsion hardware is 15 percent of propellant.

NATIONAL AERONAUTICS AND SPACE ADMINISTRATION
WASHINGTON, D.C. 20546

OFFICIAL BUSINESS
PENALTY FOR PRIVATE USE $300

SPECIAL FOURTH-CLASS RATE
BOOK

POSTAGE AND FEES PAID
NATIONAL AERONAUTICS AND
SPACE ADMINISTRATION
451

U.S.MAIL

POSTMASTER : If Undeliverable (Section 158 Postal Manual) Do Not Return

"The aeronautical and space activities of the United States shall be conducted so as to contribute . . . to the expansion of human knowledge of phenomena in the atmosphere and space. The Administration shall provide for the widest practicable and appropriate dissemination of information concerning its activities and the results thereof."

—NATIONAL AERONAUTICS AND SPACE ACT OF 1958

NASA SCIENTIFIC AND TECHNICAL PUBLICATIONS

TECHNICAL REPORTS: Scientific and technical information considered important, complete, and a lasting contribution to existing knowledge.

TECHNICAL NOTES: Information less broad in scope but nevertheless of importance as a contribution to existing knowledge.

TECHNICAL MEMORANDUMS: Information receiving limited distribution because of preliminary data, security classification, or other reasons. Also includes conference proceedings with either limited or unlimited distribution.

CONTRACTOR REPORTS: Scientific and technical information generated under a NASA contract or grant and considered an important contribution to existing knowledge.

TECHNICAL TRANSLATIONS: Information published in a foreign language considered to merit NASA distribution in English.

SPECIAL PUBLICATIONS: Information derived from or of value to NASA activities. Publications include final reports of major projects, monographs, data compilations, handbooks, sourcebooks, and special bibliographies.

TECHNOLOGY UTILIZATION PUBLICATIONS: Information on technology used by NASA that may be of particular interest in commercial and other non-aerospace applications. Publications include Tech Briefs, Technology Utilization Reports and Technology Surveys.

Details on the availability of these publications may be obtained from:

SCIENTIFIC AND TECHNICAL INFORMATION OFFICE

NATIONAL AERONAUTICS AND SPACE ADMINISTRATION

Washington, D.C. 20546